Available online at www.sciencedirect.com
SCIENCE DIRECT®
Tetrahedron Letters 45 (2004) 5081–5085
Tetrahedron Letters

Photoactive chemosensors 4: a Cu^{2+} protein cavity mimicking fluorescent chemosensor for selective Cu^{2+} recognition ☆

Sukhdeep Kaur and Subodh Kumar*

Department of Chemistry, Guru Nanak Dev University, Amritsar 143 005, India

Received 15 January 2004; revised 19 April 2004; accepted 30 April 2004

Abstract—Fluorescent chemosensor **3** can sense Cu^{2+} ions (1–8 μM) even in the presence of elevated levels of Ni^{2+}, Cd^{2+}, Zn^{2+}, Hg^{2+}, Ag^{+} and Pb^{2+} (5000 μM). **3** can also analyze for Ag^{+} ions (50–500 μM) in the presence of Ni^{2+}, Cd^{2+}, Zn^{2+}, Hg^{2+} and Pb^{2+} (5000 μM) but Cu^{2+} strongly interferes.

Amongst the soft transition metal ions, Cu^{2+} is third in abundance (after Fe^{2+} and Zn^{2+}) amongst the essential heavy metal ions in the human body and plays an important role in various biological systems. The design and synthesis of chemosensors for Cu^{2+} constitutes a very active area of research as a result of the demand for more sensitive and selective chemosensors for in vitro and in vivo purposes. Cu^{2+} is also a significant metal pollutant due to its widespread use. The Cu^{2+} toxicity for humans however is low compared to other heavy metals but certain microorganisms are affected by even submicro-molar concentrations of Cu^{2+}.[1,2]

The synthetic Cu^{2+} selective fluoroionophores so far reported[3–15] suffer from low sensitivity and, in general, higher concentrations of interfering metal ions disturb the selectivity towards Cu^{2+}. Many of these fluoroionophores have amide units as an integral part of the ionophore and Cu^{2+} is known to trigger the hydrolysis of the amide linkages[3,4] affecting the stability of these amide based sensors. Thus, the low sensitivity and high order of interference by other co-occurring metal ions has necessitated the development of new Cu^{2+} fluoroionophores.

In nature, blue copper proteins play a key role in long range inter- and intraprotein electron transfer[16,17] and are characterized by high reduction potentials, rapid transfer rates and unique spectral features compared to normal tetragonal copper complexes.[17,18] The classic type I Cu^{2+} proteins involve either four (viz two histidine, one cysteine and one methionine—amicyanin, rusticyanin, phytocyanin, plastocyanin etc.) or five coordination sites (viz two histidine, one methionine along with either two cysteines or one cysteine and one carbonyl—azurins, cytochrome C oxidase etc.)[19–21] which are arranged in distorted tetrahedral, in the case of four ligating sites, and distorted trigonal bipyramidal or distorted square pyramidal geometry, in the case of five coordination. In rusticyanin ($2 \times N + 2 \times S$), the four ligating atoms are also arranged around copper in a distorted tetrahedral arrangement but have high acid stability as the copper binding site is located within a hydrophobic region at one end of the molecule, surrounded by a number of aromatic rings and hydrophobic residues. This conformation probably contributes to the acid stability of the copper site, since the close association of aromatic rings with the histidine ligand would sterically hinder their dissociation from copper.[19b]

Bearing in mind the structural features of the active cavity in Cu^{2+} proteins in the cases of plastocyanin and rusticyanin having two N and two S binding sites and the additional stability provided by aromatic rings in the case of rusticyanin, the acyclic fluoroionophore **3**, possessing 2-aminothiophenol ($2 \times N + 2 \times S$) units as ligating sites placed on 9,10-bis(methylene)anthracene as

Keywords: Photoactive; Chemosensor; Fluorescence; Cu^{2+}.

☆ For photoactive chemosensors 1: Kumar, S.; Pramila; Kaur, S. *Tetrahedron Lett*. **2002**, *43*, 1097–1099. For photoactive chemosensors 2: Kumar, S.; Kaur, S.; Singh, G. *Supramol. Chem*. **2003**, 65–67. For photoactive chemosensors 3: see Ref. 22.

* Corresponding author. Tel.: +91-183-2556868; fax: +91-183-22588-20; e-mail: subodh_gndu@yahoo.co.in

0040-4039/$ - see front matter © 2004 Elsevier Ltd. All rights reserved.
doi:10.1016/j.tetlet.2004.04.185

the fluorophore moiety has been designed. Here, the anthracene moiety is part of the main skeleton of the fluoroionophore, and is positioned perpendicular to the ligating sites. As a result, the anthracene unit would face the cavity of the ionophore and is expected to provide a hydrophobic environment and thus high complex stability. Also in light of the participation of the anthracene appendage in cation–π interactions with an earlier reported Cu^{2+} fluoroionophore[22] the positioning of the 9,10-bis (methylene)anthracenyl ring in **3**, is expected to enhance the cation–π interactions and thus the sensitivity towards the metal ions.

The phase transfer catalyzed (K_2CO_3–DMF–TBA HSO_4) nucleophilic substitution of **1**[23] with 2-aminothiophenol **2** provided **3** as a fluorescent yellow solid (85%), mp 186 °C, MS m/z 452 (M^+) (Scheme 1). The fluoroionophore **3** in its UV–vis spectrum in CH_3CN–H_2O (4:1) shows absorption maxima (λ_{max}) at 411, 390, 371 and 303 nm.

The fluoroionophore **3** possesses two Ar-NH_2 units and undergoes protonation in the presence of acid to inhibit photoinduced electron transfer from the amine nitrogen to the excited anthracene unit. The titration of **3** (1 μM) (CH_3CN–H_2O 4:1) with acid or base shows that the fluorescence intensity of **3** remains unaffected between pH 14 and 3.8. The lowering of pH from 3.8 to 2 results in a sharp increase (nearly three times) in the fluorescence intensity. Further lowering of pH below 2 does not affect the fluorescence intensity. Therefore in the present investigation, the effect of metal ions on the fluorescence behavior of **3** has been studied at pH ~ 7 maintained with HEPES buffer (10 mM). Also, the fluorescence emission is directly proportional to the concentration of **3** in the range of 1–50 μM, therefore **3** is not susceptible to self quenching or to aggregation, at least in the concentration range explored.

In preliminary fluorescence studies, the fluoroionophore **3** (5 μM) at pH 7 (HEPES 10 mM) in CH_3CN–H_2O (4:1 v/v) in the presence of 500 mM metal ions shows fluorescence quenching with Cu^{2+} and Ag^+ only, and other metal ions viz Ni^{2+}, Cd^{2+}, Zn^{2+}, Hg^{2+} and Pb^{2+} do not affect the fluorescence of **3**. Also, the presence of alkali and alkaline earth metal ions does not affect the fluorescence of **3**. Therefore, **3** shows selective fluorescence quenching with Cu^{2+} and Ag^+ only and may be used for their quantitative estimation.

The titration of fluoroionophore **3** (5 μM) at pH 7 (HEPES 10 mM) in CH_3CN–H_2O (4:1 v/v) with Cu^{2+} nitrate exhibited a gradual decrease in the fluorescence intensity (415 nm) with increasing concentration of Cu^{2+} between 1 and 8 μM, after which the fluorescence leveled off and a plateau was achieved (Fig. 1) giving ~40% fluorescence quenching in total. Although, the other metal ions studied do not affect the fluorescence of **3** individually, except Ag^+, to explore further the utility of **3** as a Cu^{2+} selective fluoroionophore, the titration of **3** in the presence of other probable interfering metal ions has also been performed.

The plot of fluorescence of **3**-Cu^{2+} and **3**-Cu^{2+}–M^{z+} solutions versus Cu^{2+} concentration shows (Fig. 2) that the fluorescence intensity as observed in the case of the **3**-Cu^{2+} complex does not vary in the presence of 5000 μM of Ni^{2+}, Cd^{2+}, Zn^{2+}, Hg^{2+}, Ag^+ and Pb^{2+}. Therefore, **3** can estimate 1–8 μM of Cu^{2+} through fluorescence spectroscopy whilst Ni^{2+}, Cd^{2+}, Zn^{2+}, Hg^{2+}, Ag^+ and Pb^{2+} (5000 μM) do not interfere.

Since fluoroionophore **3** in its preliminary studies was also showing fluorescence quenching with Ag^+, the fluoroionophore **3** may have the ability to analyze for Ag^+. Therefore the fluorescence behavior of **3** with varied concentrations of Ag^+ has been studied and it was found that the fluorescence intensity of **3** (5 μM) showed a gradual decrease in fluorescence between 50 and 500 μM of Ag^+ and then a plateau was reached (Fig. 3). The titration of **3** in the presence of other probable interfering metal ions shows that the fluorescence of the **3**-Ag^+ complex remains unaffected in the presence of 5×10^{-3} M of Ni^{2+}, Cd^{2+}, Zn^{2+}, Hg^{2+} and Pb^{2+} as

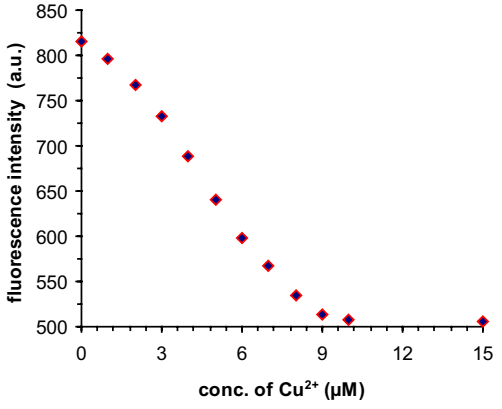

Figure 1. The fluorescence intensity versus concn of the Cu^{2+} profile of **3** at 25 ± 1 °C, pH 7 (HEPES 10 mM) in CH_3CN–H_2O (4:1). [**3**] = 5 μM, λ_{ex} = 365 nm, λ_{em} = 415 nm.

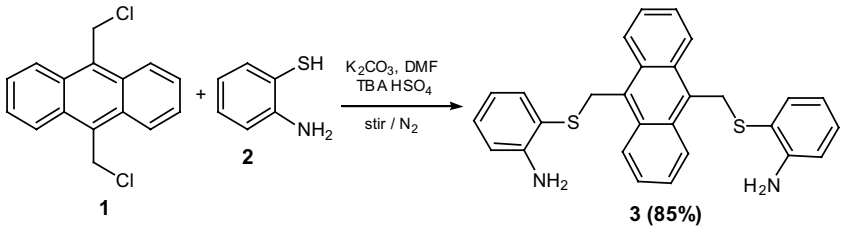

Scheme 1.

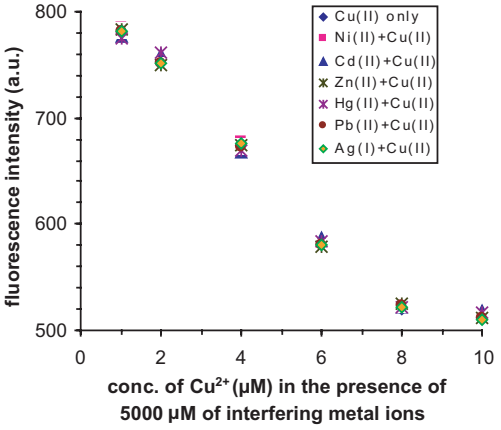

Figure 2. Estimation of Cu^{2+} in the presence of 5000 μM Ni^{2+}, Cd^{2+}, Zn^{2+}, Hg^{2+}, Ag^{+} and Pb^{2+}.

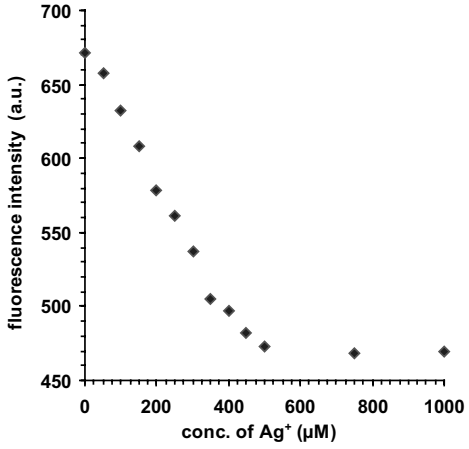

Figure 3. The fluorescence intensity versus concn of Ag^{+} profile of **3** at 25 ± 1 °C, pH 7 (HEPES 10 mM) in CH_3CN–H_2O (4:1). [**3**] = 5 μM, λ_{ex} = 365 nm, λ_{em} = 415 nm.

interfering metal ions. However the titration of **3** with Ag^{+} in the presence Cu^{2+} (5×10^{-3} M) shows enhanced quenching compared to that observed in the presence of Ag^{+} only. Therefore, Cu^{2+} strongly interferes in the estimation of Ag^{+}.

The determination of equilibrium constants for **3**-Ag^{+} and **3**-Cu^{2+} complexes give $\log K_{Ag^{+}} = 3.7 \pm 0.1$ and $\log K_{Cu^{2+}} = 5.7 \pm 0.2$, respectively. The $\log K$ values for other metal ions are very low and could not be determined. Therefore, **3** binds Cu^{2+} nearly 100 times more strongly than Ag^{+}. This higher $\log K$ with Cu^{2+} is also reflected in the noninterference of Ag^{+} in the estimation of Cu^{2+}.

To explore further the potential of **3** to act as a chromogenic sensor and the role of the anthracene moiety in π–cation interactions, the effect of metal ions on the UV–vis behaviour of **3** has been studied. In preliminary studies it was found that Ni^{2+}, Cd^{2+}, Zn^{2+}, Hg^{2+}, Ag^{+} and Pb^{2+} (20 μM) do not affect the absorption spectrum of **3** (20 μM). However on addition of Cu^{2+}, the light yellow color of the fluoroionophore disappears and a decrease in the absorbance is observed in the absorption spectrum. The titration of **3** (20 μM) in CH_3CN–H_2O (4:1) at pH ~ 7 (HEPES 10 mM) with varied concentrations of Cu^{2+} (1–200 μM) displays a linear decrease in the absorbance from 1 to 40 μM (0.1–2 equiv) and then a plateau is achieved (Figs. 4 and 5). The titration of Cu^{2+} (1–40 μM) in the presence of 20 mM concentrations of other metal ions viz Ni^{2+}, Cd^{2+}, Zn^{2+}, Hg^{2+}, Ag^{+} and Pb^{2+} has been carried out to evaluate the interference of these metal ions. The plot of absorbance of **3**-Cu^{2+} solutions and **3**-Cu^{2+}–M^{z+} solutions with respect to the concentration of Cu^{2+} present in the solution shows that the absorbance of **3**-Cu^{2+} is not affected by the presence of any of the metal ions even at 20 mM concentration (Fig. 6).

The fluorescence quenching of **3** on addition of Cu^{2+} could be attributed to the anthracene →Cu^{2+} π–cation interactions, the paramagnetic effect of Cu^{2+} and the decrease in the absorbance of **3**. Whereas, the complexation of NH_2 or -S- lone pairs of **3** with Cu^{2+} should restrict photoinduced electron transfer to the excited anthracene unit and should contribute to release of

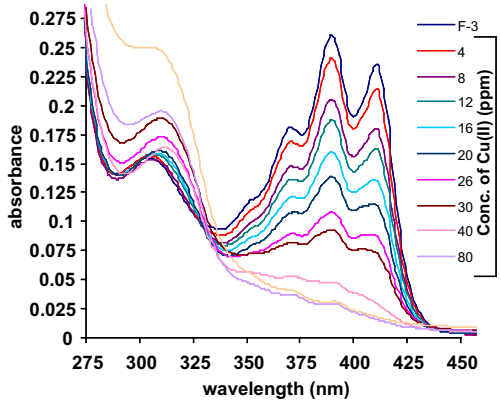

Figure 4. The effect of addition of Cu^{2+} on the absorption spectrum of fluoroionophore **3** (20 μM) at 25 ± 1 °C, pH 7 (HEPES 10 mM) in CH_3CN–H_2O (4:1).

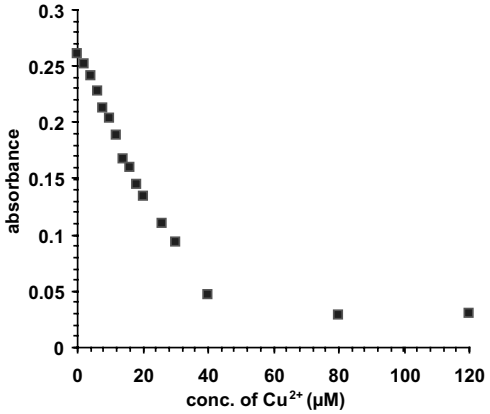

Figure 5. The absorbance versus concn of Cu^{2+} profile of **3** (20 μM) at 25 ± 1 °C, pH 7 (HEPES 10 mM) in CH_3CN–H_2O (4:1), λ_{max} = 390 nm.

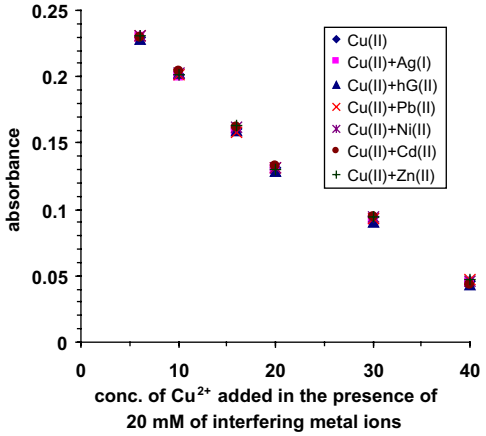

Figure 6. Estimation of Cu^{2+} in the presence of 20 mM of Ni^{2+}, Cd^{2+}, Zn^{2+}, Hg^{2+}, Ag^{+} and Pb^{2+}.

fluorescence. The addition of Cu^{2+} (2 equiv) to a solution of **3** causes an 80% decrease in the absorbance and only a 40% decrease in the fluorescence intensity. The plot of quantum yield of **3** and **3**-Cu^{2+} complex versus concentration of Cu^{2+} (Fig. 7) shows the gradual increase in quantum yield of **3** with increase in concentration of Cu^{2+}. This 2.7 times increase in fluorescence efficiency on Cu^{2+} complexation is quite close to the three times increase in fluorescence of **3** on complete protonation. Therefore amine and thioether units participate in complexation with Cu^{2+} to release the fluorescence of **3** but strong participation of anthracene in π–cation complexation results in a lowering of the absorbance of **3** and thus results in an overall decrease in fluorescence.

Thus, Cu^{2+} protein cavity mimicking fluoroionophore **3** can selectively estimate Cu^{2+} between 1 and 8 μM even in the presence of elevated levels of Ni^{2+}, Cd^{2+}, Zn^{2+}, Hg^{2+}, Ag^{+} and Pb^{2+} (5000 μM). Also, the results point to the possibility of designing a Cu^{2+} sensor with Cu^{2+} induced fluorescence enhancement by restricting the participation of the anthracene moiety in π–cation interactions or by choosing the excitation wavelength at the isobestic point around 330 nm. Investigations in this direction are under progress.

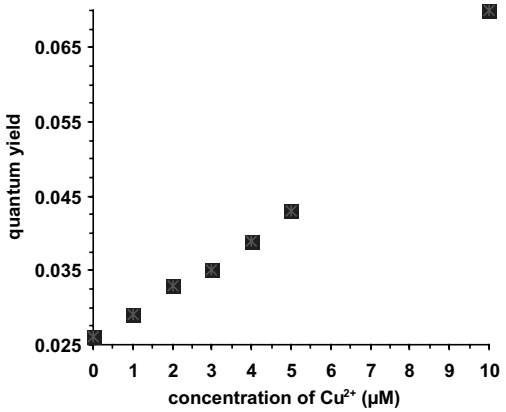

Figure 7. The plot of quantum yield of **3** and **3**-Cu^{2+} complex versus concentration of Cu^{2+} (μM) $\lambda_{ex} = 365$ nm.

Acknowledgements

We thank DST (SR/S1/OC-08/2003) New Delhi for financial assistance and the FIST programme. We also thank the referee for the useful suggestions.

References and notes

1. Lockhart, J. C. Chemical Sensors. In *Comprehensive Supramolecular Chemistry*; Gokel, G. W., Ed.; Elsevier: Pergamon, 1996; 1, pp 605–634.
2. For recent reviews: (a) Valeur, B.; Leray, I. *Coord. Chem. Rev.* **2000**, *205*, 3–40; (b) de Silva, A. P.; Fox, D. B.; Huxley, A. J. M.; Moody, T. S. *Coord. Chem. Rev.* **2000**, *205*, 41–57; (c) Prodi, L.; Bolletta, F.; Montalti, M.; Zaccheroni, N. *Coord. Chem. Rev.* **2000**, *205*, 59–83.
3. Kramer, R. *Angew. Chem., Int. Ed.* **1998**, *37*, 772–773.
4. Dujols, V.; Ford, F.; Czarnik, A. W. J. *Am. Chem. Soc.* **1997**, *119*, 7386–7387.
5. Sasaki, D. Y.; Shnek, D. R.; Pack, D. W.; Arnold, F. H. *Angew. Chem., Int. Ed. Engl.* **1995**, *34*, 905–907.
6. (a) Fabbrizzi, L.; Licchelli, M.; Pallavicini, P.; Parotti, A.; Sacchi, D. *Angew. Chem., Int. Ed. Engl.* **1994**, *33*, 1975–1977; (b) Fabbrizzi, L.; Licchelli, M.; Pallavicini, P.; Parotti, A.; Taglietti, A.; Sacchi, D. *Chem. Eur. J.* **1996**, *2*, 75–82.
7. Torrado, A.; Walkup, G. K.; Imperiali, B. *J. Am. Chem. Soc.* **1998**, *128*, 609–610.
8. Zheng, Y.; Huo, Q.; Kele, P.; Andreopoulos, F. M.; Pham, S. M.; Lablanc, R. M. *Org. Lett.* **2001**, *3*, 3277–3280.
9. Bhattacharya, S.; Thomas, M. *Tetrahedron Lett.* **2000**, *41*, 10313–10317.
10. Singh, A.; Yao, Q.; Tong, L.; Still, W. C.; Sames, D. *Tetrahedron Lett.* **2000**, *41*, 9601–9605.
11. Bodenant, B.; Weil, T.; Pourcel, M. B.; Fages, F.; Barbe, B.; Pianet, I.; Laguerre, M. *J. Org. Chem.* **1999**, *64*, 7034–7039.
12. Klein, G.; Kaufmann, D.; Schurch, S.; Reymond, J.-L. *Chem. Commun.* **2001**, 561–562.
13. Beltramello, M.; Gatos, M.; Mancin, F.; Tecilla, P.; Tonellato, U. *Tetrahedron Lett.* **2001**, *42*, 9143–9146.
14. Zhang, W.-C.; Zhu, Y.; Li, E.-C.; Liu, T.-J.; Huang, Z.-T. *Tetrahedron* **2000**, *56*, 3365–3371.
15. De Santis, G.; Fabbrizzi, L.; Licchelli, M.; Mangano, C.; Sacchi, D.; Sardone, N. *Inorg. Chim. Acta* **1997**, *257*, 69–76.
16. Solomon, E. I.; Randall, D. W.; Glaser, T. *Coord. Chem. Rev.* **2000**, *200–202*, 595–632.
17. (a) Randall, D. W.; Gamelin, D. R.; LaCroix, L. B.; Solomon, E. I. J. *Biol. Inorg. Chem.* **2000**, *5*, 16–29; (b) Adams, E. T. In *Advances in Protein Chemistry*; Anfinsen, C. B., Richards, F. M., Edsall, J. T., Eisenberg, D. S., Eds.; Academic: San Diego, 1991; 42, pp 145–197; (c) Gray, H. B.; Solomon, E. I. In *Copper Proteins*; Wiley: New York, 1981; pp 1–39; (d) Solomon, E. I.; Baldwin, M. J.; Lowery, M. D. *Chem. Rev.* **1992**, *92*, 521–542; (e) Solomon, E. I.; Lowery, M. D.; Guckert, J. A.; LaCroix, L. B. *Adv. Chem. Ser.* **1997**, *253*, 317–330.
18. Messerschmidt, A. *Struct. Bond.* **1998**, *90*, 37–68.

19. (a) Romero, A.; Nar, H.; Huber, R.; Messerschmidt, A.; Kalverda, A. P.; Canters, D. R.; Mathews, F. S. *J. Mol. Biol.* **1994**, *236*, 1196–1211; (b) Botuyan, M. V.; Toy-Palmer, A.; Chung, J.; Blake, R. C., II; Beroza, P.; Case, D. H. J. *J. Mol. Biol.* **1996**, *263*, 752–767; (c) Guss, J. M.; Merritt, E. A.; Phizackerley, R. P.; Freeman, H. C. *J. Mol. Biol.* **1996**, *262*, 686–705; (d) Guss, J. M.; Harrowell, P. R.; Murata, M.; Norris, V. A.; Freeman, H. C. *J. Mol. Biol.* **1986**, *192*, 361–387.
20. (a) Baker, E. N. *J. Mol. Biol.* **1988**, *203*, 1071–1095; (b) Hay, M.; Richards, J. H.; Lu, Y. *Proc. Natl. Sci. U.S.A.* **1996**, *93*, 461–464; (c) Kelly, M.; Lappalainen, P.; Talbo, G.; Haltia, T.; van der Oost, J.; Saraste, M. *J. Biol. Chem.* **1993**, *268*, 16781–16787; (d) Buning, C.; Comba, P. *Eur. J. Inorg. Chem.* **2000**, 1267–1273, and references cited therein.; (e) Buning, C.; Canters, G. W.; Comba, P.; Dennison, C.; Jeuken, L.; Melter, M.; Sanders-Loehr, J. *J. Am. Chem. Soc.* **2000**, *122*, 204–211, and references cited therein.
21. Basumallick, L.; Sziagyi, R. K.; Zhao, Y.; Shapleigh, J. P.; Schloes, C. P.; Solomon, E. I. *J. Am. Chem. Soc.* **2003**, *125*, 14784–14792, and references cited therein.
22. Kaur, S.; Kumar, S. *Chem. Commun.* **2002**, 2840–2841.
23. Miller, M. W.; Amidon, R. W.; Tawney, P. O. *J. Am. Chem. Soc.* **1955**, *77*, 2845–2848.